

SUPPLEMENTARY INFORMATION FOR

TITLE: NON-INVASIVE PD-L1 QUANTIFICATION USING [¹⁸F]DK222-PET IMAGING IN CANCER IMMUNOTHERAPY.

Akhilesh Mishra^{1,2}, Kuldeep Gupta¹, Dhiraj Kumar¹, Gabriela Lofland¹, Ajay Kumar Sharma¹, Lilja B. Solnes¹, Steven P. Rowe¹, Patrick M. Forde³, Martin G. Pomper^{1,3,5}, Edward W. Gabrielson^{3,4}, Sridhar Nimmagadda^{1,3,5,6*}

Author affiliations:

¹The Russell H. Morgan Department of Radiology and Radiological Science, Johns Hopkins University School of Medicine, Baltimore, MD, 21287

²Chemical & Biomolecular Engineering, Whiting School of Engineering, Johns Hopkins University, Baltimore, MD, 21218

³The Sidney Kimmel Comprehensive Cancer Center and the Bloomberg–Kimmel Institute for Cancer Immunotherapy, Johns Hopkins University School of Medicine, Baltimore, MD, 21287

⁴Department of Pathology, Johns Hopkins University School of Medicine, Baltimore, Maryland

⁵Department of Pharmacology and Molecular Sciences, Johns Hopkins University School of Medicine, Baltimore, MD, 21287

⁶Division of Clinical Pharmacology, Department of Medicine, Johns Hopkins University School of Medicine, Baltimore, MD, 21287, USA.

Correspondence: Sridhar Nimmagadda, Ph.D.
Johns Hopkins Medical Institutions
1550 Orleans Street, CRB II, #492
Baltimore, MD 21287
Phone: 410-502-6244
Fax: 410-614-3147
Email: snimmag1@jhmi.edu

Data availability statement

All data relevant to the study are included in the article, uploaded as online supplementary information. All data are available on reasonable request.

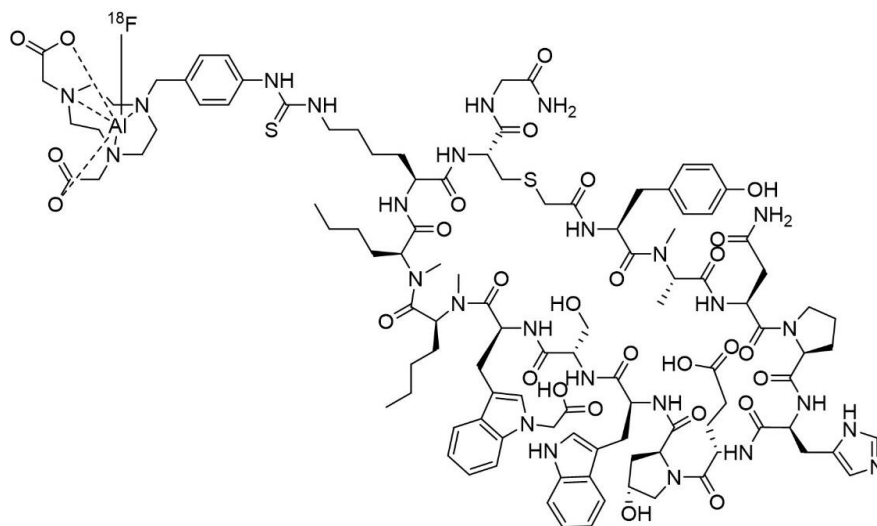


Figure S1. Structure of [^{18}F]DK222

Cell Line	Cancer type	RNASeq Score
		$\log_2(\text{TPM}+1)$
H2444	Lung Cancer	5.349
H226	Lung Cancer	3.875
A549	Lung Cancer	1.791
BFTC909	Urothelial Cancer	7.775
T24	Urothelial Cancer	4.259
SCABER	Urothelial Cancer	3.175

Table S1. $\log_2(\text{TPM}+1)$ gene expression data extracted from Cancer Cell Line Encyclopedia for cell lines used in this study.

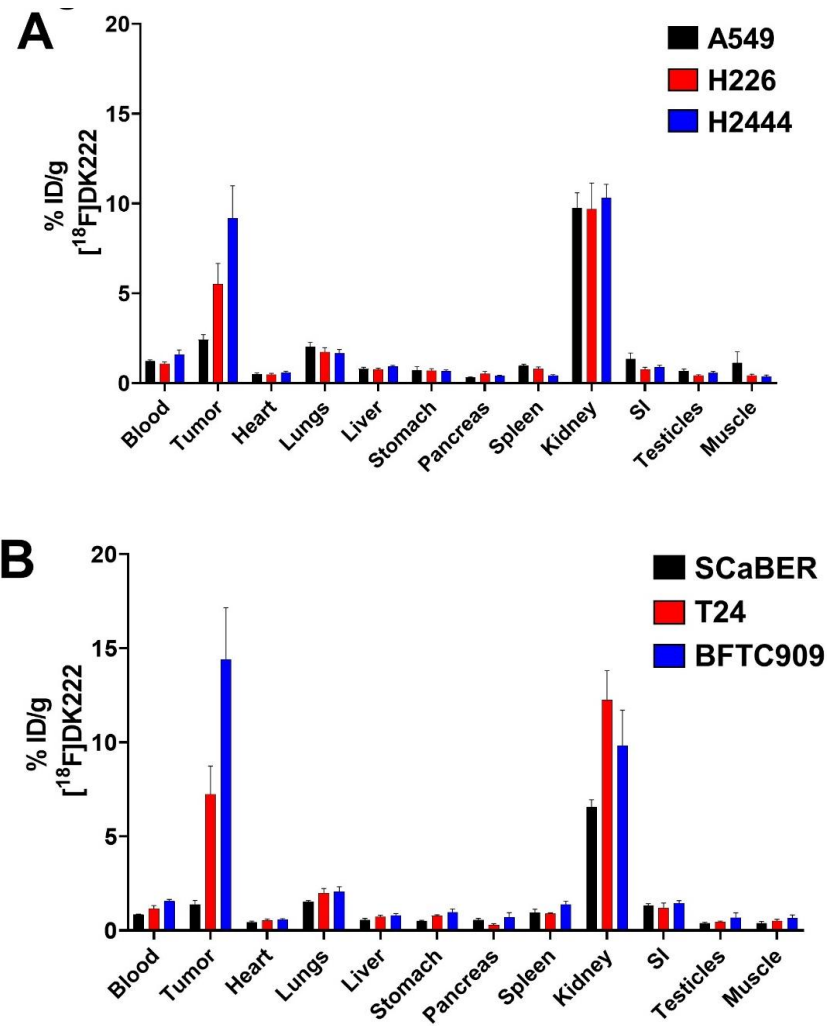


Figure S2. Ex vivo biodistribution in NSG mice bearing (A) NSCLC or (B) UC xenografts. Mice were injected with ~ 740 kBq (~20 μCi) $[^{18}\text{F}]$ DK222 in 200 μL of 5% ethanol in saline and sacrificed after 60 minutes ($n=5$).

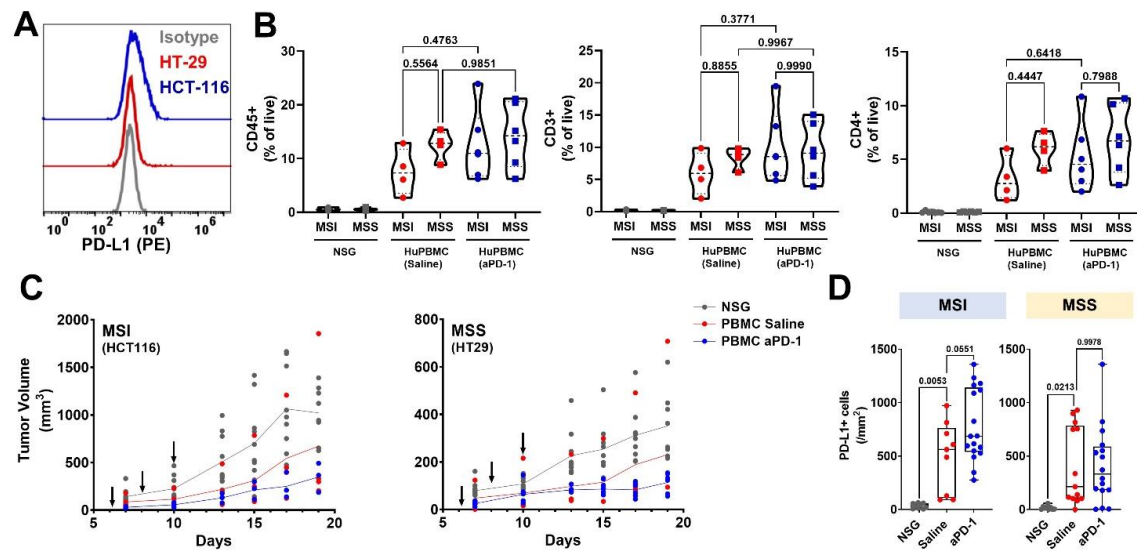


Figure S3. Flow cytometry analysis of MSI (HCT-116) and MSS (HT-29) tumors by flow cytometry. **A**, Baseline PD-L1 expression in MSI (HCT-116) and MSS (HT-29) cell lines. **B**, CD45+ immune cells, CD3+T cells and CD4+ T cells in tumors engrafted in huPBMC or NSG mice with and without aPD-1 treatment (4 mg/kg pembrolizumab *i.v.* on day 4, 6 and 8 as indicated by arrows). **B**, Tumor growth curves for MSI (HCT-116) and MSS (HT-29) tumors treated with either 4 mg/kg pembrolizumab *i.v.* on day 4, 6 and 8 or saline. P values by two-way ANOVA

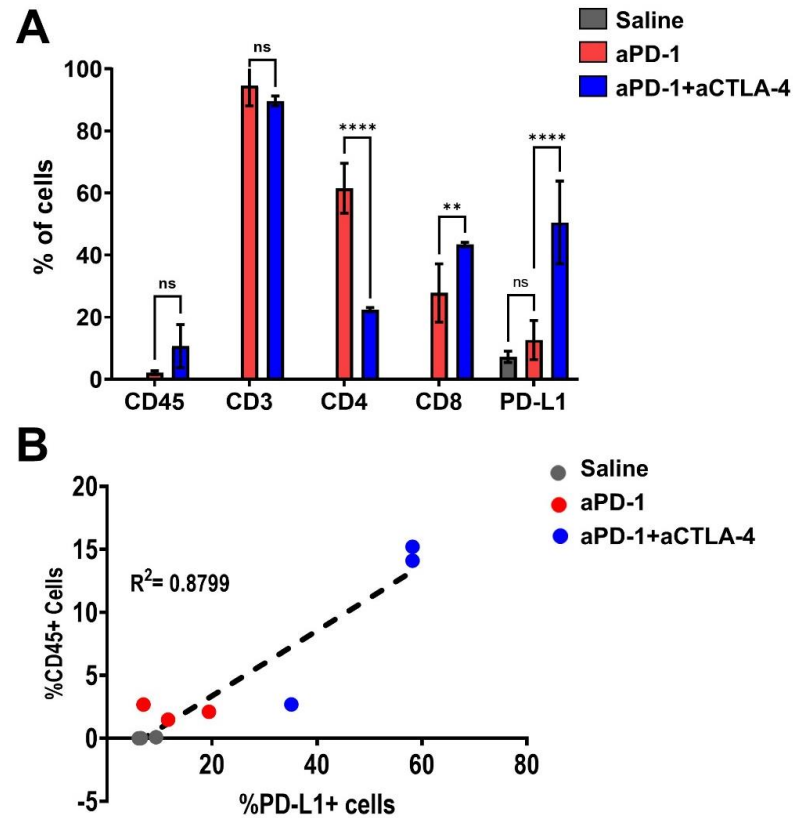


Figure S4. Flow cytometry data for A375 tumors engrafted in humanized mice (huCD34). **A**, Flow cytometry histograms showing increased immune cell infiltration and upregulated PD-L1 expression tumors of mice treated with different immunotherapy or saline. **B**, Immune cell analysis shows strong correlation between CD45+ immune cell infiltration and PD-L1 expression on tumor cells. ** $p < 0.01$, **** $p < 0.0001$ by two-way ANOVA

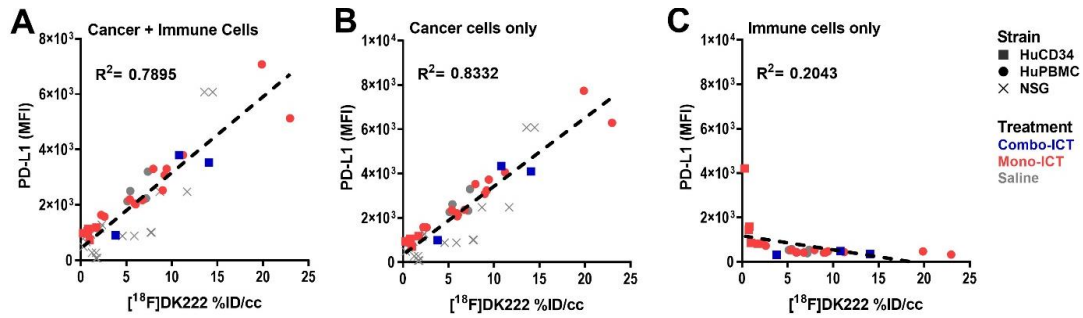
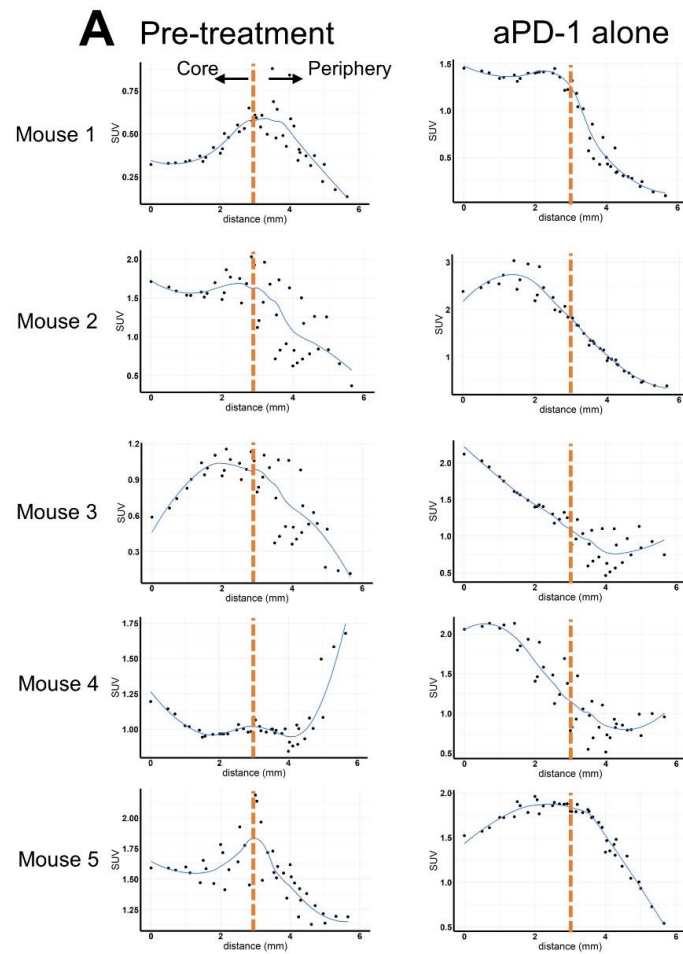


Figure S5. Combined correlation of all data points in different studies used in **Figure 5**. Flow cytometry derived PD-L1 MFI on **(A)** all cells, **(B)** cancer cells alone or **(C)** immune cells alone was used to correlate with $[^{18}\text{F}]\text{DK222}$ %ID/cc on corresponding PET datasets. Simple linear regression and Pearson coefficient were used.

Figure S6



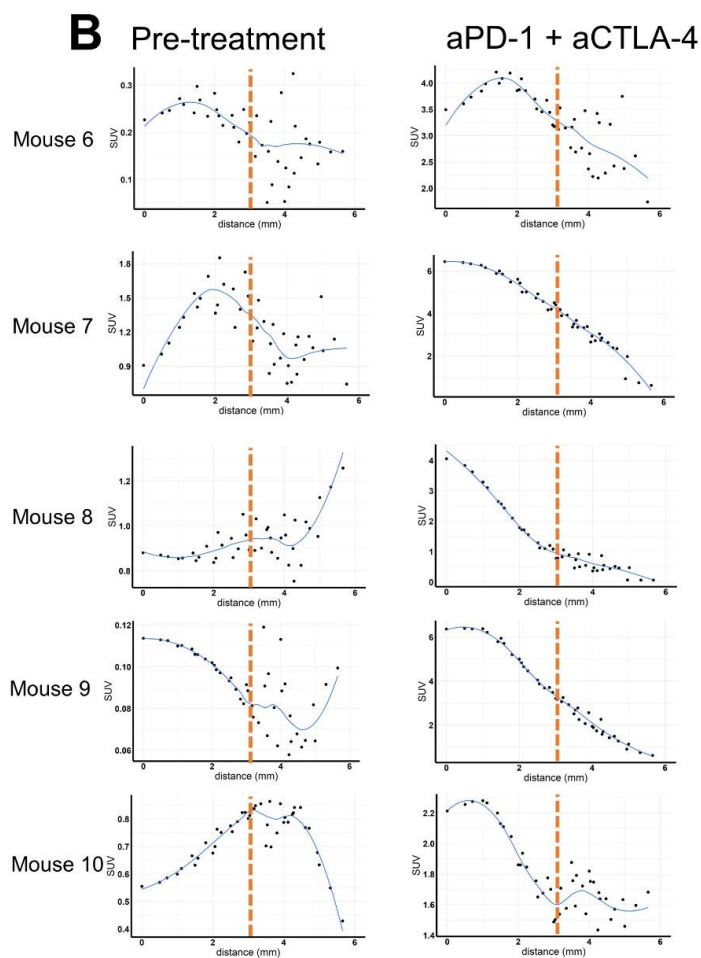


Figure S6 Individual SUV [18 F]DK222 vs distance of each mice before and after mono- **(A)** or combination-treatment **(B)**.

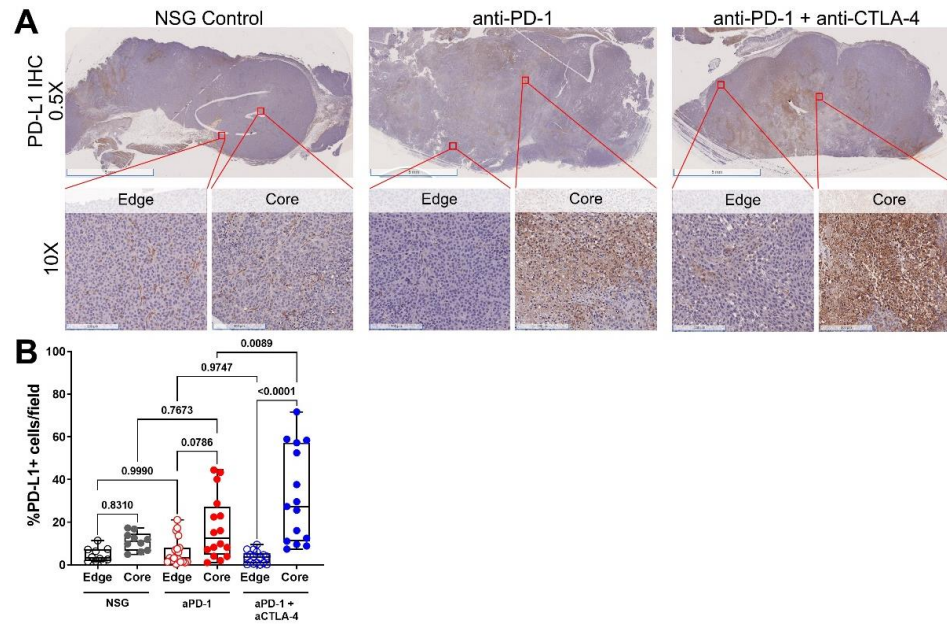


Figure S7. A, Representative PD-L1 immunohistochemistry of A375 tumors treated with aPD-1 monotherapy or aPD-1+aCTLA-4 combination therapy. **B:** Quantification of immunoreactivity for PD-L1 at edges and cores of tumors treated with mono- or combination therapy.